Monitoring the species-specific absorption of solar energy by chlorophyll through near-surface imaging spectroscopy in central eastern Amazon

Cibele Hummel do Amaral [1]
Luiz Eduardo Oliveira e Cruz de Aragão [2]
Lênio Soares Galvão [2]
Jin Wu [3]
Thomas Hilker [4, †]
Yhasmin Mendes Moura [2]
Neill Prohaska [5]
Scott Saleska [5]

[1] Universidade Federal de Viçosa - UFV/DEF
36570-900 - Viçosa - MG, Brazil
chamaral@ufv.br

[2] Instituto Nacional de Pesquisas Espaciais – INPE/DSR
12245-970 - São José dos Campos - SP, Brazil
{luiz.aragao, lenio.galvao}@inpe.br, yhas.mendes@gmail.com

[3] Brookhaven National Laboratory - BNL/EE Dept.
11973-5000 PO Box 5000 - Upton - NY, United States
jinwu@bnl.gov

[4] University of Southampton - SOTON
SO17 1BJ - Southampton - HPH, United Kingdom
t.hilker@soton.ac.uk

[5] University of Arizona – UofA/EEB
85721 - Tucson - AZ, United States
photosynthesis@gmail.com, saleska@email.arizona.edu

[†] *In memoriam*

Abstract. The aim of this research was to monitor the amount of solar energy absorbed by chlorophyll at branch scale during the dry season, in a central eastern Amazonian evergreen forest, and verify how broadband and narrowband vegetation indices, as well as canopy fractions can be used for monitoring the absorption of energy by chlorophyll at the species level. Seventeen hyperspectral images (385-1050 nm, ~ 4 nm spectral resolution), which were acquired from a tower-mounted camera (late July to late September, 2012), were used in this study. Seven vegetation indices, three canopy fractions (green vegetation, GV, non-photosynthetic vegetation, NPV, and shade fractions), and the depth of the chlorophyll absorption band, were calculated for three tree species in the camera image: *Chamaecrista xinguensis* (CHXI), *Erisma uncinatum* (ERUN) and *Manilkara huberi* (MAHU). Each individual (and species) displays a distinct phenological behavior, and ERUN has the highest values and the lowest variation of chlorophyll absorption band depth during the studied period. Our results show that the dry season changes in chlorophyll absorption band depth are not correlated with the shade fraction; instead, it can be explained by the dry season variations in GV and NPV, as well as by three vegetation indices: Normalized Difference Vegetation Index (NDVI), Enhanced Vegetation Index (EVI) and Plant Senescence Reflectance Index (PSRI). Although NDVI and EVI are more consistent during the time, only NDVI and PSRI are correlated with the absorption of the electromagnetic energy by chlorophyll within the studied crowns (and species).

Palavras-chave: Amazon, temporal analysis, chlorophyll absorption band, spectrometry, vegetation indices, spectral mixture analysis.

1. Introduction

Remote sensing plays a crucial role in studying climate-vegetation interactions around the world. Except the difficulty of collecting data from tropical forests in the field, remote sensing would allow us to analyze forests across multiple scales, from finer crown/canopy scales (Lopes et al., 2016) up to broader landscape and regional/global scales (Higgins et al., 2014; Guan et al., 2015). Ambient environments as carbon dioxide, water and light are essential for plant photosynthesis, and their seasonality might cause temporal variation in forest canopy photosynthetic capacity due to certain evolutionary adaptive strategies. Thus, several remote sensing studies have long been interested in exploring how seasonal and inter-annual variability in environments (e.g. light and water) affect the variability in forest photosynthetic capacity in the tropics (e.g., Huete et al., 2006; Saleska et al. 2007; Asner & Alencar, 2010; Samanta et al., 2010; Morton et al., 2014; Guan et al., 2015). Nevertheless, modeling photosynthetic capacity of the Amazon forest from space based on those factors is still challenging.

Trees respond in a species-specific manner to exchange carbon dioxide with ambient environment (Ozanne et al., 2003), and the high biodiversity of Amazonian trees makes it extremely difficult to use a generic model to estimate canopy photosynthetic capacity from finer crown scale up to regional and global scales. Edaphic factors are also known to drive species composition in the Amazon (e.g., Tuomisto et al., 2003; Higgins et al., 2011 and 2014). Thus, any floristic variation limited by edaphic factors will also reflect changes in broader landscape, regional estimations of photosynthetic capacity. In this context, remote sensing studies at finer scales (i.e. using near-surface and field sensors) and comprising different species communities of the Amazon forest must be done.

Recent studies based on a tower-mounted imaging system and a field reflectance spectroscopy have shown that species-specific leaf age, development and demography are important mechanisms responsible for Amazon canopies' photosynthetic capacity in response to seasonal light and rainfall variations (e.g., Wu et al., 2016; Chavana-Bryant et al., 2016). These studies also demonstrate the importance of hyperspectral measurements for addressing this challenge through remote sensing.

Using hyperspectral images from an Amazonian evergreen forest canopy, this research aimed to track the species-specific amount of solar energy absorbed by chlorophyll at branch scale during the 2012 dry season. By considering the light-dependent reactions crucial to capture carbon dioxide and complete the photosynthesis, we use the variations in depth of the chlorophyll absorption band for monitoring the species' photosynthetic capacity at branch scale. We also verified how broadband and narrowband vegetation indices, as well as canopy fractions can be used for monitoring the absorption of energy by chlorophyll at the species level.

2. Material and Methods
2.1. Material

The studied canopy is located around 2°51'19.4" S and 54°57'33.5" W, at Km 67 site in the Tapajós National Forest (Belterra, PA, Brazil) (**Figure 1**). It is characterized as Dense Tropical Forest of high plateau, according to RADAMBRASIL (1976). The sampled species are *Chamaecrista xinguensis* (CHXI), *Erisma uncinatum* (ERUN) and *Manilkara huberi* (MAHU); they were sensed by the tower-mounted Hyperspectral Vegetation Imaging System (HVIS) with a 45˚ view angle. According to IBAMA (2004) CHXI is the most abundant species in the Tapajós National Forest (6.3 individuals/hectare), followed by MAHU (4.0 ind./ha) and ERUN (1.1 ind./ha).
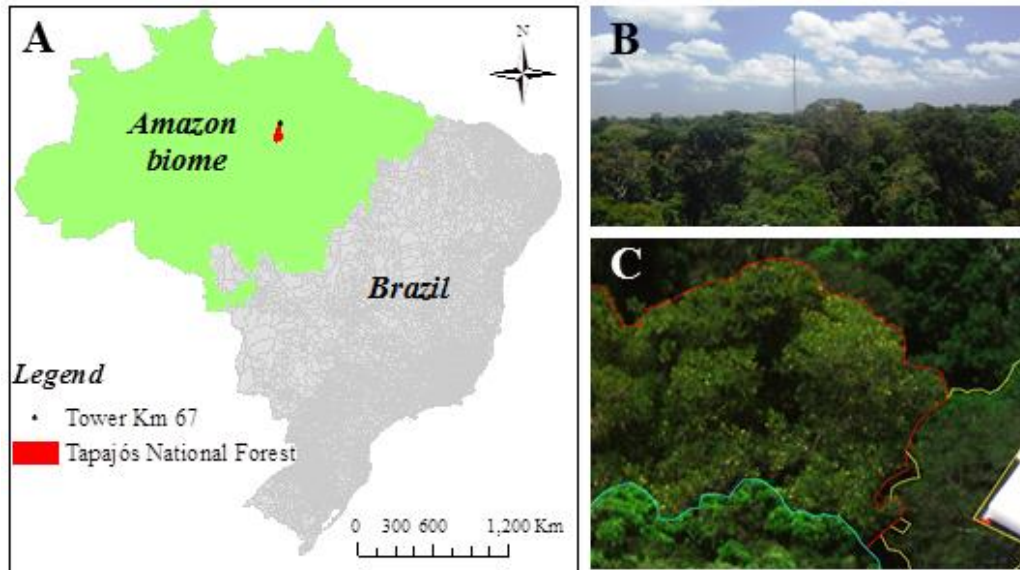
Figure 1. Location of the tower-based Hyperspectral System at Tapajós National Forest (Km 67) in the Brazilian Amazon biome (A), side view of the tower on the canopy (B), and hyperspectral image, highlighting the species crowns: *Chamaecrista xinguensis* (outlined in yellow), *Erisma uncinatum* (cyan) and *Manilkara huberi* (red) (C). Source: Brazilian Institute of Geography and Statistics – IBGE.

The monthly variations of Photosynthetically Active Radiation (PAR) and of rainfall express the seasonality of inputs for photosynthetic processes and atmosphere-biosphere gas exchanges at the study site. The period of study (from July to September) is historically characterized by a PAR increase and a rainfall decrease (**Figure 2**).
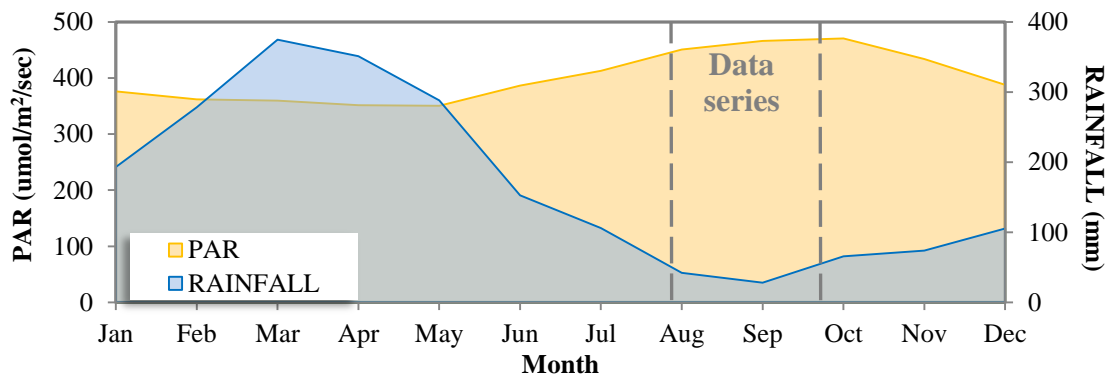
Figure 2. 2002-2011 monthly averages: Photosynthetically Active Radiation – PAR (umol/m^2/sec) from Eddy Flux tower, at km 67 site, Tapajós National Forest (PA); and Rainfall (mm) from Belterra (PA) station. Highlight for the seasonal period covered by the imagery, collected in 2012. Source: National Institute of Meteorology – INMET.

The hyperspectral images were collected by a tower-monted Hyperspectral Vegetation Imaging System (HVIS) – SOC710 (Surface Optics Corporation, San Diego - CA, USA), from ~ 65 m height. The system provides spectral coverage from 385 to 1050 nm, with ~ 4 nm of spectral resolution, and instantaneous field of view of 36 x 27 degrees. With temporal resolution of one hour, the system acquired during the days several images with view zenith angles of ~ 15°, 30°, 45°, 60° and 75°. The entire dataset comprises hundreds of images from July to December, 2012.

2.2. Methods
2.2.1. Hyperspectral data series selection and calibration

First, the datasets from July to December, 2012 were analyzed, in order to retain for processing only those data collected as closer as possible to solar-noon, as well as containing a surface (plate) of reference for reflectance retrieval. 23 scenes were retained for processing; they were collected at 11:21AM with 45° view angle, from the end of July to the end of September, 2012 (Day of Year – DOY: 210-268). By considering the influence of variations in solar radiation and cloud cover on the signal obtained, the solar irradiance data were analyzed from the reference plate in the images, in order to set a series standardized and with the highest illumination conditions. Finally, 17 images of the series were held for processing. The relative reflectance per wavelength was retrieved through the ratio between the digital number of the pixels and the digital number of the plate.

2.2.2. Data processing

Seven vegetation indices related to canopy structure, leaf area, leaf pigments and leaf physiology were calculated from the images. They are the Normalized Difference Vegetation Index (NDVI), Enhanced Vegetation Index (EVI), Anthocyanin Reflectance Index 1 (ARI1), Carotenoid Reflectance Index (CRI), Photochemical Reflectance Index (PRI) and Plant Senescence Reflectance Index (PSRI) (**Table 1**).

Tabela 1. Vegetation indices calculated for seasonal analysis at branch scale from three tree species of the Tapajós National Forest, PA, Brazil: A) biophysical, B) biochemical e C) physiological.

Index		Formula	Reference
A	**NDVI**	$(\rho864 - \rho671) / (\rho864 + \rho671)$	Rouse et al. (1973)
	EVI	$(\rho864 - \rho671) / (1 + \rho864 + 6 \cdot \rho671 - 7.5 \cdot \rho467) \cdot 2.5$	Huete et al. (2002)
B	**ARI1**	$(1/\rho550) - (1/\rho700)$	Gitelson et al. (2001)
	CRI	$(1/\rho508) - (1/\rho701)$	Gitelson et al. (2002)
C	**PRI**	$(\rho529 - \rho569) / (\rho529 + \rho569)$	Gamon et al. (1997)
	PSRI	$(\rho681 – \rho498) / \rho752$	Merzlyak et al. (1999)

Additionally, Multiple Endmember Spectral Mixture Analysis (MESMA; Roberts et al., 2007) was performed on the 17 reflectance images. MESMA generates linear models using various sets of endmembers from spectral libraries, and selects the model with the lowest RMSE for each pixel (Roberts et al., 1998). Fraction images of green vegetation (GV), non-photosynthetic vegetation (NPV) and shade were generated for the 17 dates, by using ViperTools (Roberts et al., 2007).

In order to verify how vegetation indices and canopy fractions can explain the variations in chlorophyll absorption band depth, spectrometric analyses were performed after continuum removal. The continuum is removed from segments of the spectrum to normalize the differences in brightness while highlighting the absorption features present in the interval (Clark and Roush, 1984). The depth of the chlorophyll absorption band – located around 680 nm – in the continuum removed spectra were calculated using the Processing Routines in IDL for Spectroscopic Measurements (PRISM; Kokaly, 2011). Three branches were randomly selected within all three crowns. No distinction among sun and shade's leaves, and leaves' age has been done. From those regions of interest, time series from the spectral indices, fraction images, and chlorophyll absorption band depth were generated, and correlation analyses between them were performed. The fittest regression type and the coefficient of determination from each regression analysis are presented.

3. Results and Discussion

The seasonal variation of the chlorophyll absorption band depth from *Chamaecrista xinguensis* (CHXI), *Erisma uncinatum* (ERUN) and *Manilkara huberi* (MAHU), at branch scale, from DOY 210 to 268 (peak of the dry season) is shown in the **Figure 3**. ERUN branches presented the lowest chlorophyll absorption band depth's variation as well as the deepest chlorophyll absorption features during the time. At the branches 1 and 3, chlorophyll slightly decreases around DOY 215-217, followed by a greening event right after. At the same time, branches 1 and 3, mainly, of MAHU shows the highest chlorophyll increasing. This species appears to simultaneously experience old leaves senescence and new leaves sprouting. CHXI branches seem to be less sensitive to that event, around DOY 215-217. They present the highest chlorophyll decrease between DOY 226 and 246 (interval with no data). This is caused by a massive leaf fall which can clearly be seen in the true color, fractions and vegetation index images (**Figure 4**).
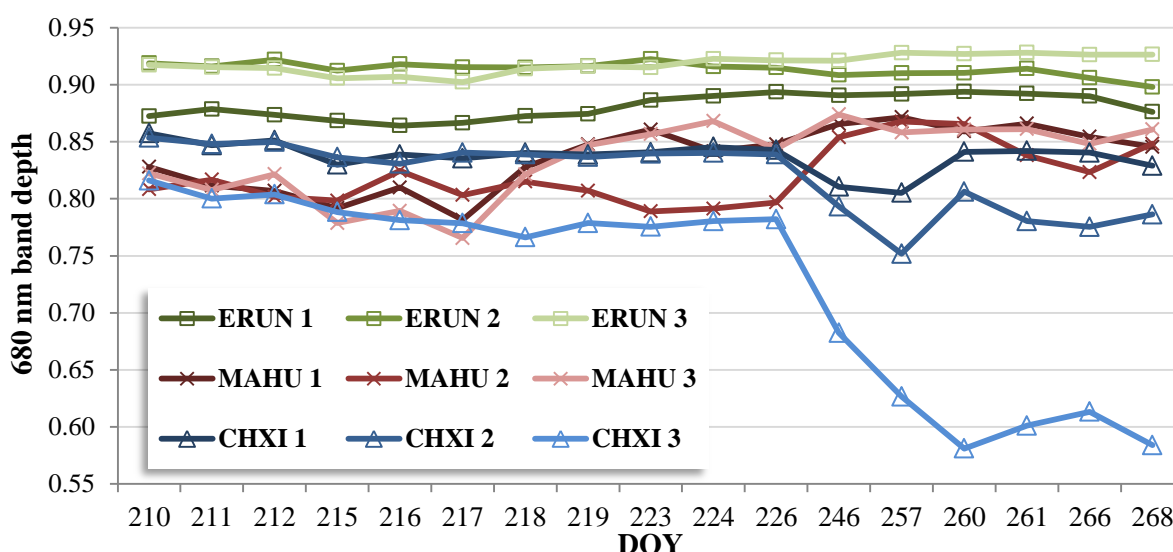
Figure 3. Variation in chlorophyll absorption band depth from DOY 210 to 268, from three random branches of *Erisma uncinatum* (ERUN), *Manilkara huberi* (MAHU) and *Chamaecrista xinguensis* (CHXI) at Tapajós National Forest, PA, Brazil.
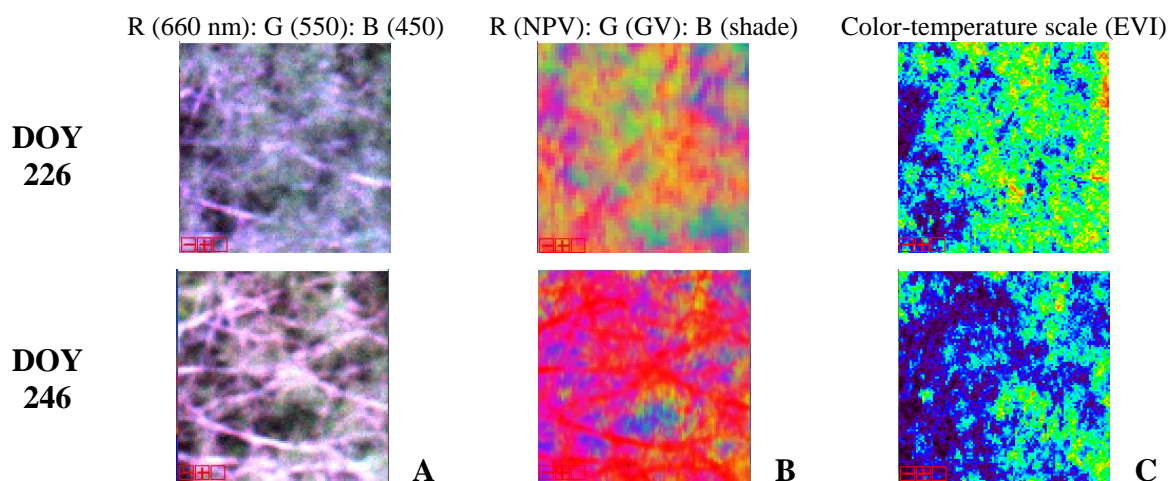

Figure 4. True-color RGB composition (A), non-photosynthetic vegetation (NPV), green vegetation (GV) and shade fractions in RGB composition (B), and Enhanced Vegetation Index (EVI) in color-temperature scale, scaled from low-values (blue) to high-values (red), showing leaf fall in a branch of *Chamaecrista xinguensis* from DOY 226 to 246.

The absence of correlation between chlorophyll absorption band depth and shade fraction ($R^2 = 0.159$) shows the potential of using the first one to analyze the sensitivity of spectral indices for estimating the amount of energy absorbed by chlorophyll in the canopies and their seasonal trends. Green vegetation (GV) and Non-photosynthetic vegetation (NPV) fractions were correlated to the chlorophyll absorption band depth, and only NDVI, EVI and PSRI presented high correlation with that metric at branch scale (**Table 2**). In general, GV showed to be the worst metric to explain the variations in chlorophyll absorption band depth; its performance varies differently between months and species. In opposite, NPV presented high negative correlation with the chlorophyll absorption band depth (R = 0.807).

Table 2. Correlation between sub-pixel canopy fractions (GV and NPV) and vegetation indices (NDVI, EVI, and PSRI) (y) with chlorophyll absorption band depth (x) at branch scale: coefficient of determination (R^2) for the entire dataset, by month and by species (ERUN, MAHU, and CHXI).

| Regression Y Axis	Type (slope)	R^2	R^2 by month			R^2 by species		
			July	August	September	ERUN	MAHU	CHXI
GV	Exponential (+)	0.717	0.407	0.574	0.826	0.001	0.104	0.830
NPV	Pol. 2rd Order (-)	0.807	0.662	0.668	0.878	0.179	0.657	0.876
NDVI	Pol. 2rd Order (+)	0.982	0.967	0.977	0.993	0.894	0.913	0.990
EVI	Pol. 2rd Order (+)	0.860	0.829	0.882	0.873	0.496	0.563	0.595
PSRI	Pol. 2rd Order (-)	0.812	0.767	0.752	0.941	0.896	0.806	0.949

Although NDVI is known by its issues related to the signal saturation on canopies with high biomass (Huete et al., 2002), it presented the highest correlation with the chlorophyll absorption band depth, as expected, followed by EVI. Both regression shapes (**Figure 5**) explained the higher NDVI sensitivity to changes in chlorophyll, and the higher EVI sensitivity to variations in leaf area and canopy structure (Gao et al., 2000). Both indices also perform well when the data series is subdivided by month (smaller periods), which is not observed for the other analyzed metrics.
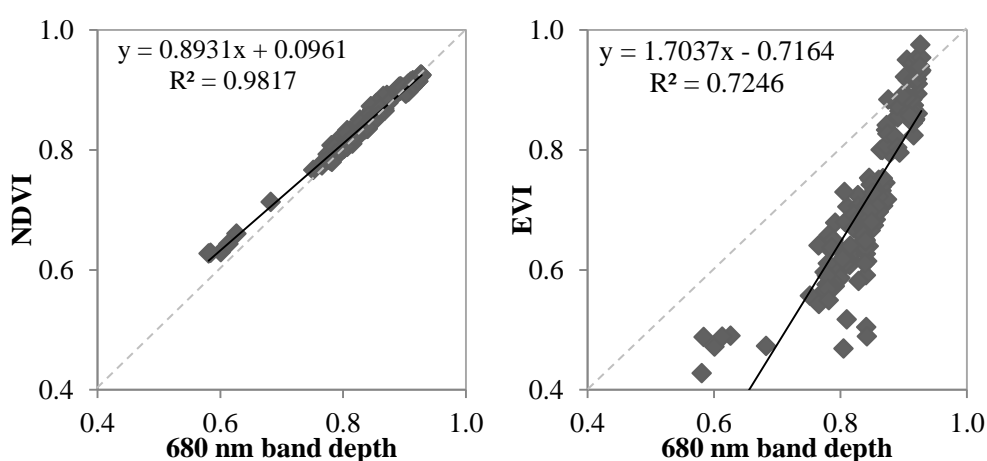
Figure 5. Linear relationship between NDVI (Normalized Difference Vegetation Index) and EVI (Enhanced Vegetation Index) with the depth of the chlorophyll absorption band (680 nm) at branch scale, from three tree species from DOY 210 to 268 at Tapajós National Forest, PA, Brazil.

GV did not present any relationship with the seasonal variations of chlorophyll absorption band depth from ERUN and MAHU branches (**Figure 6**). They are two of the most representative species of the Tapajós National Forest canopy (Espírito-Santo et al, 2005). NPV showed to be a good metric for estimating species-specific absorption of energy by chlorophyll, except for ERUN which showed the highest values and the lowest variation of chlorophyll absorption band depths. As NDVI, PSRI also performed well when the data series

was analyzed by species (**Figure 6**); it performed better than EVI for species-specific chlorophyll estimations. PSRI is known to be sensitive to the carotenes/chlorophylls ratio, and can be used for estimating leaf senescence (Merzlyak et al., 1999). Differently from the other analyzed indices, PSRI is the unique to use the signal from the red edge spectral region.
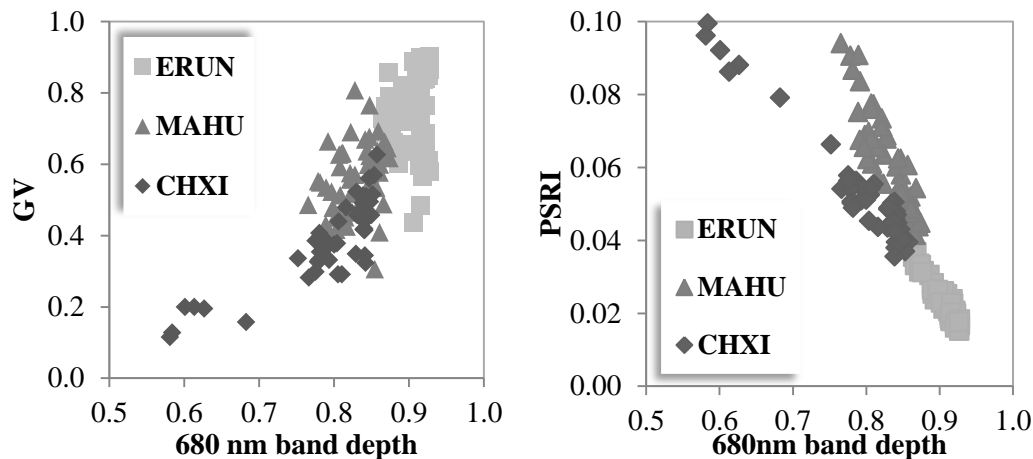
Figure 6. Species-specific relationship between Green-vegetation fraction (GV) and Plant Senescence Reflectance Index (PSRI) with the depth of the chlorophyll absorption band (680 nm) at branch scale, from DOY 210 to 268 at Tapajós National Forest, PA, Brazil. ERUN = *Erisma uncinatum*, MAHU = *Manilkara huberi*, and CHXI = *Chamaecrista xinguensis*.

4. Conclusions

Each sampled individual (and species) at the Tapajós National Forest displays a distinct phenological behavior at branch scale from July to September, 2012. *Manilkara huberi* (MAHU) and *Chamaecrista xinguensis* (CHXI), which show leaf senescence, leaf fall and leaf sprouting during the studied period, have also higher within-crown spectral variability than *Erisma uncinatum* (ERUN). ERUN shows the highest values and the lowest variation of chlorophyll absorption band depth during the peak of the dry season.

The seasonal changes of the chlorophyll absorption band depth are not correlated to the seasonal variation in shade fraction. Instead, it can be explained by the variations of the photosynthetic (GV) and non-photosynthetic (NPV) vegetation, as well as by the NDVI, EVI and PSRI variations when analyzed the entire dataset. NDVI and EVI are also more consistent during the time; they explain well ($R^2 \geq 0.829$) the variations of the chlorophyll absorption band depth even when the dataset is analyzed by month.

GV and NPV fractions are more species-specific dependent than the analyzed vegetation indices. The highest correlations of the chlorophyll absorption band depths with the canopy fractions and the vegetation indices are observed for the deciduous species (CHXI). EVI did not explain as well in the seasonal variability in chlorophyll absorption band depth of CHXI branches ($R^2 = 0.595$), compared with GV ($R^2 = 0.830$).The variations of the chlorophyll absorption band depth from the evergreen (and more representative) sampled species, ERUN and MAHU, are not explained by the changes in GV, NPV and EVI and in GV and EVI, respectively. NDVI and PSRI are suitable for monitoring changes in energy absorbed by chlorophyll, during DOY 210-268 (peak of the dry season), within the studied crowns (and species) from the Dense Tropical Forest of high plateau, at the Tapajós National Forest.

Acknowledgements

References

Asner, G., Alencar, A. Drought impacts on the Amazon forest: the remote sensing perspective. **New phytologist**, v.187, p.569-578, 2010.

Chavana-Bryant, C., Malhi, Y., Wu, J., Asner, G. P., Anastasiou, A., Enquist, B. J., ... Martin, R. E. Leaf aging of Amazonian canopy trees as revealed by spectral and physiochemical measurements. **New Phytologist**, n.13853, p.1-15, 2016.

Clark, R. N., Roush, T. L. Reflectance spectroscopy: Quantitative analysis techniques for remote sensing applications. **Journal of Geophysical Research**, v. 89, p. 6329-6340, 1984.

Espírito-Santo, F. D. B., Shimabukuro, Y. E., Aragão, L. E. O. C., Machado, E. L. M.. Análise da composição florística e fitossociológica da floresta nacional do Tapajós com o apoio geográfico de imagens de satélites. **Acta Amazonica**, v.35, n.2, p.155-173, 2005.

Gamon, A., Serrano, L., Surfus, S. The photochemical reflectance index : an optical indicator of photosynthetic radiation use efficiency across species, functional types, and nutrient levels. **Oecologia**, v.112, p.492–501, 1997.

Gao, X., Huete, A. R., Ni, W., Miura, T. Optical–biophysical relationships of vegetation spectra without background contamination. **Remote Sensing of Environment**, v. 74, p. 609- 620, 2000.

Gitelson, A.A., Merzlyak, M.N., Chivkunova, O.B. Optical properties and nondestructive estimation of anthocyanin content in plant leaves. **Photochemistry and Photobiology**, v. 74, n.1, p. 38-45, 2001.

Gitelson, A.A., Zur, Y., Chivkunova, O.B., Merzlyak, M.N. Assessing Carotenoid Content in Plant Leaves with Reflectance Spectroscopy. **Photochemistry and Photobiology**, v.75, n.3, p. 272-281, 2002.

Guan, K., Pan, M., Li, H., Wolf, A., Wu, J., Medvigy, D., Caylor, K.K., Sheffield, J., Wood, E.F., Malhi, Y., Liang, M. Photosynthetic seasonality of global tropical forests constrained by hydroclimate. **Nature Geoscience**, v.8, n.4, p.284-289, 2015.

Higgins, M. A., Asner, G. P., Perez, E., Elespuru, N., Alonso, A. Variation in photosynthetic and nonphotosynthetic vegetation along edaphic and compositional gradients in northwestern Amazonia. **Biogeosciences**, v.11, n.3, p.3505-3513, 2014.

Huete, A. R., Didan, K., Shimabukuro, Y. E., Ratana, P., Saleska, S. R., Hutyra, L. R., ... Myneni, R. Amazon rainforests green-up with sunlight in dry season. **Geophysical research letters**, v.33, n.6, L06405, p.1-4, 2006.

Huete, A., Didan, K., Miura, T., Rodriguez, E. P., Gao, X., Ferreira, L. G. Overview of the radiometric and biophysical performance of the MODIS vegetation indices. **Remote sensing of environment**, v.83, n.1, p.195-213, 2002.

Instituto Brasileiro do Meio Ambiente e dos Recursos Naturais Renováveis – IBAMA. **Floresta Nacional do Tapajós**: Plano de manejo – vol.1. Available at http://www.icmbio.gov.br/portal/images/stories/imgs-unidades-coservacao/flona_tapajoss.pdf. Accessed in 05 Feb. 2016.

Kokaly, R. F. **PRISM**: Processing routines in IDL for spectroscopic measurements. Denver: U.S. Geological Survey, 2011. Available at http://pubs.usgs.gov/of/2011/1155/. Accessed in 12 Jan. 2013.

Lopes, A.P., Nelson, B.W., Wu, J., de Alencastro Graça, P.M.L., Tavares, J.V., Prohaska, N., Martins, G.A. Saleska, S.R. Leaf flush drives dry season green-up of the Central Amazon. **Remote Sensing of Environment**, v. 182, p.90-98, 2016.

Merzlyak, M. N., Gitelson, A. A., Chivkunova, O. B., Rakitin, V. Y. (1999). Non-destructive optical detection of pigment changes during leaf senescence and fruit ripening. Physiologia Plantarum, 106, 135-141.

Morton, D. C., Nagol, J., Carabajal, C. C., Rosette, J., Palace, M., Cook, B. D., ... North, P. R. Amazon forests maintain consistent canopy structure and greenness during the dry season. **Nature**, v.506, n.7487, p.221-224, 2014.

Ozanne, C. M. P., Anhuf, D., Boulter, S. L., Keller, M., Kitching, R. L., Körner, C., ... Stork, N. E. Biodiversity meets the atmosphere: a global view of forest canopies. **Science**, v.301, n.5630, p.183-186, 2003.

Roberts, D. A., Gardner, M., Church, R., Ustin, S., Scheer, G., Green, R. O. Mapping Chaparral in the Santa Monica Mountains using multiple endmember spectral mixture models. **Remote Sensing of Environment**, v.65, p.267-279, 1998.

Roberts, D. A., Halligan, K. Q., Dennison, P. E. **VIPER Tools**: user manual version 1.5. 2007. Available at http://www.vipertools.org/. Accessed in 17 Feb. 2013.

Rouse Jr, J., Haas, R. H., Schell, J. A., Deering, D. W. Monitoring vegetation systems in the Great Plains with ERTS. **NASA special publication**, v.351, p.309-317, 1974.

Saleska, S. R., Didan, K., Huete, A. R., da Rocha, H. R. Amazon forests green-up during 2005 drought. Science, v.318, n.5850, p.612-612, 2007.

Samanta, A., Ganguly, S., Hashimoto, H., Devadiga, S., Vermote, E., Knyazikhin, Y., ... Myneni, R. B. (2010). Amazon forests did not green-up during the 2005 drought. **Geophysical research letters**, v.37, L05401, p.1-5, 2010.

Wu, J., Albert, L. P., Lopes, A. P., Restrepo-Coupe, N., Hayek, M., Wiedemann, K. T., ... Tavares, J. V. Leaf development and demography explain photosynthetic seasonality in Amazon evergreen forests. **Science**, v. 351, n. 6276, p. 972-976, 2016.